



## ***Chapter-6***

***To encapsulate the bioactive  
compounds extracted from  
haritaki using a combination  
of biopolymeric materials***

## 6.1. Introduction

Haritaki is a very famous rejuvenating herb, and a medium to large-sized tree distributed throughout tropical and subtropical Asia, including China, Bangladesh, Bhutan and Tibet. As a result, the food and flavour industries are looking for novel food components to use in the development of food supplements. The consumption of haritaki may also aid in the fulfilment of nutritional needs and the prevention of many degenerative illnesses such as cancer, neurological and cardiovascular disorders, ageing, and so on [27]. The economic worth of the raw material and the profitability of the haritaki processing could both increase with the extraction of the beneficial chemicals found in the pulp. The use of bioactive chemical extracts in food items is nevertheless subject to a number of restrictions, including their limited stability, which is altered by solvents, pH, temperature, oxygen, light, and enzymes.

Encapsulation is described as a process that surrounds small particles or droplets with a coating or embeds them in a homogeneous or heterogeneous matrix to produce small capsules with a variety of useful properties [25, 26]. Encapsulation is used in this context to increase the stability of these compounds and protect them from harmful Operations for freeze-drying are more significant in this situation. However, because these processes take place under various time and temperature conditions, the resulting products have varying qualities [26]. These techniques are frequently used to microencapsulate residue extracts and other bioactive substances from natural sources, such as phenolic compounds from the peels of pomegranate (*Punica granatum L.*) and grape (*Vitis labrusca var. Bordo*) and jaboticaba (*Myrciaria jaboticaba*) and blackberry (*Rubus fruticosus*) and grape pomace [47, 44].

The capacity to form films, biodegradability, gastrointestinal tract resistance, viscosity, solids content, hygroscopicity, and cost should all be taken into consideration when using different encapsulating agents, both individually and in combination [47]. Bioactive substances have been encapsulated using a variety of techniques using food-grade polymers and proteins [3]. Zein, a protein found in corn that is alcohol-soluble and high in prolamine, is one of them. Three parts of the amino acids are lipophilic, while one portion is hydrophilic [16]. This material provides better biodegradability, mechanical properties, tolerance to high temperature, film formation capability, biological compatibility, barrier towards moisture and oxygen, thereby making it useful for

encapsulating lipophilic bioactive chemicals [19]. As per sources, zein protein is stable for up to 120 min in a simulated stomach environment, but becomes unstable in less than 30 sec in a simulated intestinal environment. This demonstrated that zein would improve the bio-accessibility of the bioactive chemical by increasing its protection against gastric circumstances and encouraging release of the compound only in intestinal fluid [18]. By using a phase separation approach and drying in a rotary evaporator to create powder, Jain et al. [22] used zein nanoparticles for encapsulating carotene, thereby achieving regulated administration and improved pharmacokinetic properties. Oil and surfactants have also been employed as carriers for lipophilic compounds in addition to zein [20].

There have been some studies on the microencapsulation of fruit and plant extracts that have been published. These studies discuss the antioxidant compounds [36, 37], storage stability [36, 37], physico-chemical properties [36]. A report on acerola pomace extracts microencapsulated, and on the physical characteristics was published by Moreira et al. [33] respectively. However, no research on the microencapsulation of the bioactive components from haritaki pulp has yet been published. Therefore, the purpose of this work was to freeze-dry and conventionally encapsulate bioactive chemical extracts from agro-industrial haritaki pulp, as well as to identify the physical, bioactive compound, thermal, and morphological features of the dried products.

## **6.2. Materials and methods**

### **6.2.1. Material**

Haritaki was collected from the horticulture section of Tezpur University, Assam, India. Chemicals of the analytical grade required for the current study were purchased from Himedia in Mumbai, India.

### **6.2.2. Extraction of bioactive compounds from haritaki**

The fruit was cleaned, and the pulp and seed were separated. A laboratory tray dryer (Labotech, BDI-51, B. D. Instrumentation, Ambala, India) was used for the drying of pulp at 40 °C. After this, the dried pulp was crushed and put through a 100-mesh screen before being sealed in polythene bags with an aluminium laminate until further usage. The supercritical fluid extractor vessel (Applied Separations, USA) was filled with the powdered haritaki pulp (1 g), and the extracts were then collected in the glass tubes of

separator. The extraction conditions of the phytochemicals were similar to our previous study [23].

### **6.2.3. Encapsulation of bioactive compounds**

#### **6.2.3.1. Conventional technique**

Through the use of an encapsulator, sodium alginate was used to capsule the extract (Buchi B-390, India). Using a magnetic stirrer, 4 g of sodium alginate was slowly added to distilled water (100 mL) and forcefully stirred (1,500 rpm) until it was entirely dissolved. The combination was then given 10 mL of the extract, which was then extruded via an encapsulator (300 µm nozzle size) into a solution of 2% CaCl<sub>2</sub>, stirred continuously using a glass rod, and stored (4 °C) for further analysis [31].

#### **6.2.3.2. Advanced technique**

In order to produce the haritaki encapsulate using the advanced technique, different combinations of hydrocolloids were prepared to increase the yield and encapsulation of bioactive constituents. Potato starch and zein was mixed in the ratio of 0:100, 30:70, 50:50, 70:30, and 100:0 (w/w) in the water and heated at 80 °C for 10 min on hot-plate magnetic stirrer (AI-022, Alfa instruments, India) at 560 rpm. The prepared mixture was kept in a freeze dryer (-86 °C, Lyolab, India) 24 h at a pressure of 5 mm Hg. Porous solids that had been created were pulverised in a mortar and pestle, put through a sieve with a mesh size of 25, and then immediately put into glass containers with screw-on lids and kept in a freezer (-18 °C).

### **6.2.4. Characterization of physical properties of encapsulates**

#### **6.2.4.1. Moisture content and water activity**

The AOAC 18th ed. technique was used to determine the moisture content of freeze-dried powder (925.10). An electronic dew point water activity meter (Aqualab Series 4TE, Decagon Devices, Inc., Pullman, Washington, USA) was used to determine the water activity of the powder.

#### **6.2.4.2. Process yield (PY)**

The amount of powder collected after freeze drying to the original amount of the feed solutions was used as the gravimetric measure of the process yield of the powder [15].

$$PY (\%) = \frac{\text{Mass of Powder Collected}}{\text{Mass of solid fed}} \times 100 \quad (6.1)$$

#### 6.2.4.3. Encapsulation efficiency

The haritaki's encapsulation efficiency was determined by dividing the amount of encapsulated haritaki by the amount of total extract in the freeze-dried powder. Using the same organic solvent (petroleum ether), surface extract was likewise extracted, however at room temperature as opposed to a higher temperature. This approach was taken from Botrel and colleagues [9]. Powdered haritaki (5 g) in capsules was steeped in 75.0 mL of petroleum ether (1:15 w/v, as in hot pentane Soxhlet extraction) in a conical flask. To help wash the powder from the oleoresin on the surface, the flask was occasionally swirled. Filtered petroleum ether was then mixed with an equivalent volume of new solvent, and the process was carried out three times. Petroleum ether was then collected, filtered, evaporated at 40 °C under vacuum, and finally, under a steady stream of nitrogen, until all of the remaining solvent was evaporated. Weighing the extractable surface haritaki (WSO), its percentage was also determined. The percentage was calculated using the mean and standard deviation of three determinations  $\pm$ SD.

$$\text{Encapsulation Efficiency (EE}_L \text{ \%)} = \frac{W_{TO} - W_{SO}}{W_{TO}} \times 100 \quad (6.2)$$

Where, EE<sub>L</sub>: the effectiveness of haritaki's encapsulation, W<sub>TO</sub>: weight of the total haritaki computed in a sample of powder (based on a 1:4 weight ratio of haritaki to powder in the initial formulation of the emulsion), W<sub>SO</sub>: weight of the extractable surface haritaki extract empirically discovered in the same weight of powder.

#### 6.2.5. Packing and flow properties

The mass per unit volume of a bed of loose powder is known as the bulk density. The particle envelope volumes and the gaps between the particles are both included in the unit volume. The mass-to-volume ratio of a powder after it has been tapped for a specific amount of time is known as the powder's "tapped density." A powder's tapped density is an accurate representation of its dense packing. The average mass of the particles divided by the volume of the solid, excluding all voids that are not essential to the molecular packing arrangement, is the true density of a material. Bulk density and tapped density of powder were measured as per Santhalakshmy et al. [43].

$$\text{Bulk density} = \frac{\text{Weight of the powder (g)}}{\text{Total volume of powder}} \quad (6.3)$$

$$\text{Tapped density} = \frac{\text{Weight of the powder (g)}}{\text{Total volume of powder after tapping}} \quad (6.4)$$

Powder cohesiveness, often measured by the Hausner ratio and equation 5, was used to calculate it, while equation 6 opted to calculate the Carr's Index of powder.

$$\text{Hausner ratio} = \frac{\text{Tapped Density}}{\text{Bulk Density}} \quad (6.5)$$

$$\text{Carr's Index} = \frac{\text{Tapped Density} - \text{Bulk Density}}{\text{Tapped Density}} \times 100\% \quad (6.6)$$

### **6.2.6. Colour properties**

The colour properties were calculated as discussed in section 3.2.9 [3].

### **6.2.7. Fourier transform infrared spectroscopy (FT-IR) spectra**

The Fourier transform infrared spectroscopy (FT-IR) spectra was calculated as discussed in section 5.2.5 [7].

### **6.2.8. Surface morphology**

The surface morphologies of the encapsulates were examined using a scanning electron microscope (SEM) (JEOL JSM 6700F) at 500-2000× magnification [46].

### **6.2.9. Thermodynamic properties**

#### **6.2.9.1. Differential scanning calorimetry**

Using Differential Scanning Calorimetry (DSC TA-Q20), the thermal stability of freeze-dried encapsulate was examined. To do this, water (14 mL) was poured with a micro syringe to the freeze-dried encapsulate (10 mg db) in the DSC pans, which was then sealed and reweighed. The samples were heated at a rate of 10 °C/min while being scanned from 35 °C to 150 °C with an empty aluminium pan serving as the reference. Using the software Universal Analysis 2000 3.9A, parameters including onset, peak, final, and gelatinization temperatures were determined from the thermographs of the samples [50].

#### **6.2.9.2. Thermo-gravimetric analysis (TGA)**

A Mettler-Toledo TGA/SDTA851E was used to calculate the mass loss of the freeze-dried encapsulation. The sample mass (6 mg) was kept constant during the test

while temperatures between 30 °C and 500 °C were administered at a heating rate of 10 °C/min under nitrogen [24].

### 6.2.10. Statistical analysis

In the present study, IBM SPSS Statistics Version 20.0, Armonk, NY: IBM Corporation package was used for the statistical analysis of data, and the means were separated using Duncan's multiple range test ( $p < 0.05$ ). All the data were presented as the mean with the standard deviation.

## 6.3. Result and Discussion

### 6.3.1. Encapsulation of bioactive compounds using conventional and advanced method

The bioactive compounds from haritaki pulp powder were extracted using SFE and was encapsulated via conventional methods (alginate-matrix) and advanced methods (freeze-drying). **Fig. 6.1** and **6.2** represents the encapsulates prepared from the different techniques. Freeze dried microcapsules were prepared using the different ratio of potato starch and zein (0:100; 30:70; 50:50; 70:30; 100:0) where the certain problems were arisen during the mixing of starch and zein powder due to their hydrophobic nature.

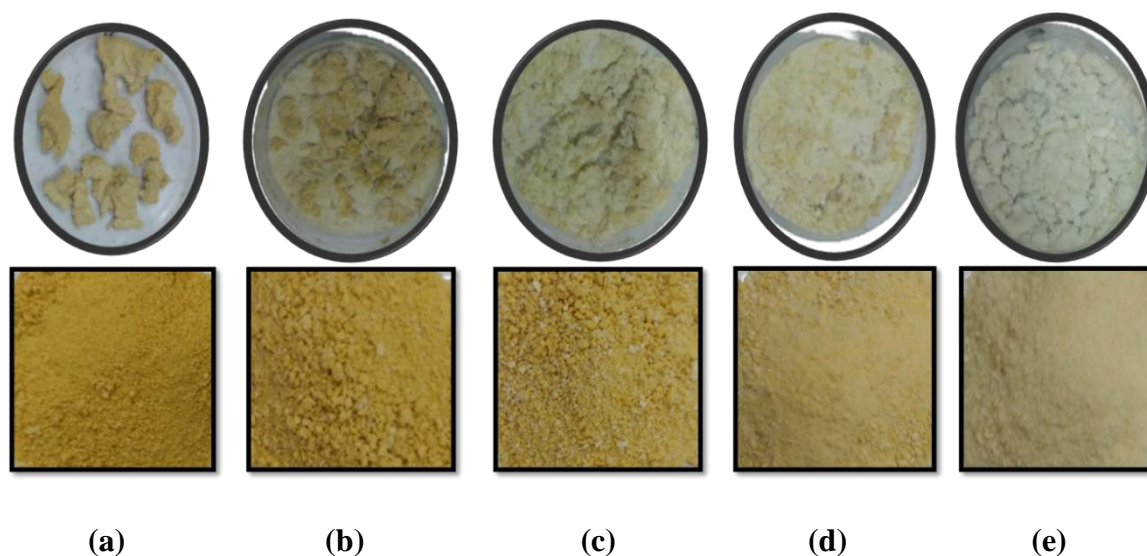


**Fig. 6.1.** Haritaki encapsulates obtained from freeze-drying (a) starch:zein (0:100) (b) starch:zein (30:70) (c) starch:zein (50:50) (d) starch:zein (70:30) (e) starch:zein (100:0)

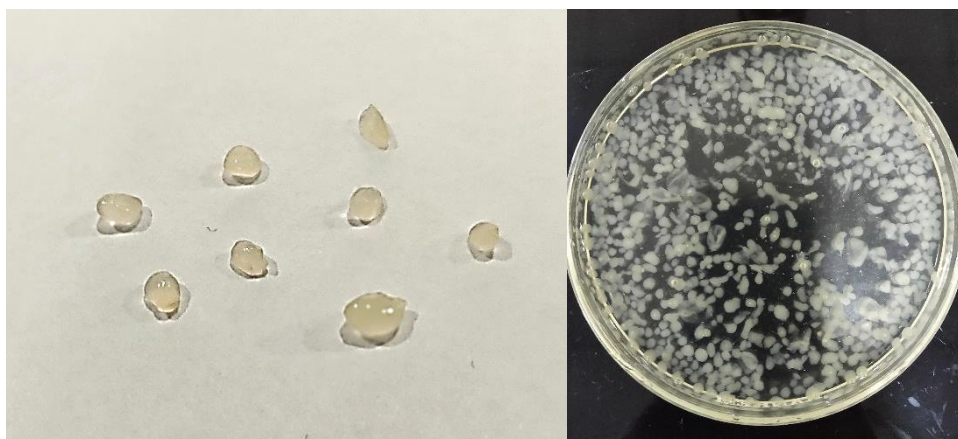


**Fig. 6.2.** Encapsulation of bioactive compounds via encapsulator

Zein protein also don't form a homogenous mixture when heated with water along with varied proportion of starch. Although, it is been reported that, zein is an excellent matrix to develop capsules, as well as improved bioavailability in simulated gastrointestinal tract and so on. In the present investigation, it was observed that 100% zein did not able to produce the good quality of phytochemicals loaded capsules while the 100% potato starch has successfully produced the capsule which is attributed to high solubility, and biocompatible nature of starch. It has already been established that, potato starch is an excellent binder, tableting excipients, disintegrant, matrix former and release retardant agents [35]. Encapsulates produced from the both techniques were compared in terms of yield and encapsulation efficiency of phytochemicals. Based on the results, it was noted that, alginate encapsulated capsules had the lower yield (53.90%) and encapsulation efficiency (56.06%) of phytochemicals than the encapsulates prepared from freeze-drying technique (65.45% & 75.95% of yield and encapsulation efficiency respectively). Thus, freeze dried encapsulates were selected for the further characterization study.

### **6.3.2. Characterization of physical properties of encapsulates**

#### **6.3.2.1. Process yield and Encapsulation efficiency**

The maximum yield of the encapsulate was observed in case of 100% starch followed by 70:30, 50:50, 30:70, and 0:100 starch: zein respectively. Thus, the encapsulates with 100% starch showed that the materials for the walls have good film-forming capabilities, with ratios of 70:30, and 50:50 presented a good interaction than 100% zein [4]. As it is reported that, starch is a common material in pharmaceutical applications due to its biocompatible and biodegradable, cheap and available in large quantities. Besides, phytochemicals encapsulate with higher zein in the composition



achieved lower process yield, suggesting that the increased concentration of Zein did not exhibit very good film-formation ability.

The efficacy of encapsulation varied in-between 43.86-75.95% where it was shown that the phytochemicals with zein and starch at ratios of 70:30, 50:50, 30:70, and 0:100 possessed noticeable difference. The maximum encapsulation was achieved with 100% of starch indicating the excellent film forming properties of starch than zein. But the opposite results were reported by Zhang et al. [53]. The authors encapsulated capsaicin through the use of whey protein and modified starch, where microcapsules having high percentage of modified starch in their composition attained lesser encapsulation than whey protein. These results were conquering with encapsulation of phytosterol (efficiency 96.2%) done with spray drying in which Gum Arabic and maltodextrin were used. Encapsulation efficiency relies on few factors such as emulsion formulation and type of wall materials [15].

#### **6.3.2.2. Moisture content and water activity**

Moisture content of powder depicts a significant role in estimating flow behaviour, shelf stability and cohesive nature [43]. The moisture level of the capsules was between 6% and 7.32%, which is slightly greater than the 4% minimum requirement for powder used in the food business. Agglomeration lowers the scattering of active substances, prevents microbial development, microcapsules with lesser humidity can result in the reduction of mildew degradation and moisture absorption, enhancing the physical and chemical stability. For dry powders, water activity ( $a_w$ ) is a quantitative index whose value is used to determine the food system's shelf life (**Table 6.1**). Water activity of the samples ranged from 0.32 to 0.50, indicating that the encapsulates will be stable for a longer period of time [51].

#### **6.3.2.3. Bulk, and Tapped density**

Bulk, tapped, and true density are the important characteristic features of powder. There was a significant difference ( $p < 0.05$ ) in the encapsulated powder. Highest bulk density was shown by E (100% starch) while lowest was observed in (B) (starch:zein (30:70)) and (C) (starch:zein (50:50)). Freeze drying treatment might have caused intense depolymerization of the macromolecules which results in decreased or increased value of bulk density [6]. Powders with more bulk density require less volume for packaging and vice-versa. The similar results were noticed in the tapped density of encapsulates.

### 6.3.2.4. Carr's index and Hausner ratio

Carr's index and Hausner ratio are interrelated and calculated from the information of bulk and tapped densities (**Table 6.1**). There was a significant difference ( $p < 0.05$ ) between the samples. The physical properties of encapsulates were also affected by freeze-drying treatment and caused increase or decrease in flow behaviour with increased dosage of zein & starch. The Carr's index of the encapsulates prepared from 100% zein (A) had shown a very low value while the encapsulate prepared from 70:30 (starch:zein) had a very high value. Based on the results it can be assumed that 100% zein encapsulates has excellent flowability than the other encapsulates. The lower Carr's index of samples that were freeze and spray dried could be attributed to the higher moisture content, which makes particles adhere together and increases flow resistance. It could also be because these microcapsules are tiny and have an uneven shape [38].

**Table 6.1.** Physical properties of freeze dried encapsulate

Parameters	A	B	C	D	E
<b>Bulk density (g/cm<sup>3</sup>)</b>	0.48±0.01 <sup>b</sup>	0.29±0.00 <sup>d</sup>	0.29±0.00 <sup>d</sup>	0.34±0.00 <sup>c</sup>	0.61±0.01 <sup>a</sup>
<b>Tapped density (g/cm<sup>3</sup>)</b>	0.51±0.00 <sup>b</sup>	0.35±0.00 <sup>d</sup>	0.35±0.00 <sup>d</sup>	0.42±0.00 <sup>c</sup>	0.72±0.01 <sup>a</sup>
<b>Carr's Index (%)</b>	7.14±2.15 <sup>c</sup>	17.55±1.23 <sup>ab</sup>	15.88±1.83 <sup>ab</sup>	18.47±1.63 <sup>a</sup>	14.42±1.68 <sup>b</sup>
<b>Hausner ratio (%)</b>	1.07±0.02 <sup>c</sup>	1.21±0.01 <sup>ab</sup>	1.18±0.02 <sup>ab</sup>	1.22±0.02 <sup>a</sup>	1.16±0.02 <sup>b</sup>
<b>a<sub>w</sub></b>	0.32±0.01 <sup>e</sup>	0.50±0.00 <sup>a</sup>	0.42±0.01 <sup>b</sup>	0.40±0.00 <sup>c</sup>	0.37±0.01 <sup>d</sup>
<b>Moisture (%)</b>	6.03±0.06 <sup>e</sup>	6.44±0.05 <sup>c</sup>	6.28±0.04 <sup>d</sup>	6.85±0.06 <sup>b</sup>	7.32±0.04 <sup>a</sup>
<b>Encapsulation efficiency (%)</b>	43.86±2.72 <sup>d</sup>	51.50±0.17 <sup>c</sup>	55.36±1.80 <sup>c</sup>	63.42±0.43 <sup>b</sup>	75.95±0.88 <sup>a</sup>
<b>Yield (%)</b>	46.71±2.85 <sup>d</sup>	49.92±0.29 <sup>cd</sup>	51.86±1.66 <sup>bc</sup>	53.95±0.29 <sup>b</sup>	65.45±2.58 <sup>a</sup>
<b>L*</b>	82.72±0.96 <sup>c</sup>	85.39±0.41 <sup>b</sup>	80.90±1.67 <sup>c</sup>	76.44±1.22 <sup>d</sup>	96.67±1.09 <sup>a</sup>
<b>a*</b>	2.01±0.22 <sup>c</sup>	1.21±0.13 <sup>d</sup>	2.91±0.53 <sup>b</sup>	5.09±0.58 <sup>a</sup>	-1.15±0.31 <sup>e</sup>
<b>b*</b>	24.49±1.26 <sup>c</sup>	21.70±0.35 <sup>d</sup>	28.43±1.27 <sup>b</sup>	30.33±0.86 <sup>a</sup>	6.96±0.21 <sup>e</sup>

Values are means ± standard deviation of three determinations (n = 5). Values followed by different superscript letter in a row are significantly different ( $p \leq 0.05$ ).

Higher Hausner ratio was recorded in the case of 70:30 (starch:zein) near to 1.25, while 100% zein encapsulates has shown the value of 1.07, which indicate that encapsulates from 70:30 (starch:zein) has poor flowability while 100% zein encapsulates possesses good flowing index.

### **6.3.3. Colour properties**

Colour property is an important parameter to assess the acceptability of powder. In the present study, colour parameters such as  $L^*$ ,  $a^*$  and  $b^*$  values were calculated for the freeze dried encapsulates and the results are summarized in **Table 6.1**. There was significant difference among the samples were noticed due to the different composition. Highest  $L^*$  was recorded by (E) (100 % starch) followed by (D) (70:30 (starch:zein)) and the least value was seen in (B) (30:70 (starch:zein)). The highest lightness in E attributes to usage of 100% starch. In case of  $a^*$  value, the encapsulates produced by 70:30 (starch:zein) had the maximum followed by 50:50 (starch:zein) while the minimum value was recorded by 100% starch. The colour characteristics may have been significantly affected by the encapsulation produced v/s freeze drying, and variations were associated with the browning response and the reassociation of amylose at higher temperatures [39]. On the other hand,  $b^*$  value represents yellow to blue tinge of food product, that is also noticed to significantly affected by combination and freeze drying of encapsulates. Encapsulate prepared by 70:30 (starch:zein) had a higher value while the minimum value was seen in 100 % starch encapsulates.

### **6.3.4. Surface morphology of powder**

The surface morphologies of the freeze dried encapsulates are presented in **Fig. 6.3**. From illustration it can be observed that, due to the partial collapse of the polymeric gel network, the encapsulates contained rough, uneven microparticles with heterogeneous surface morphologies that were indicative of materials that had been dried [5].

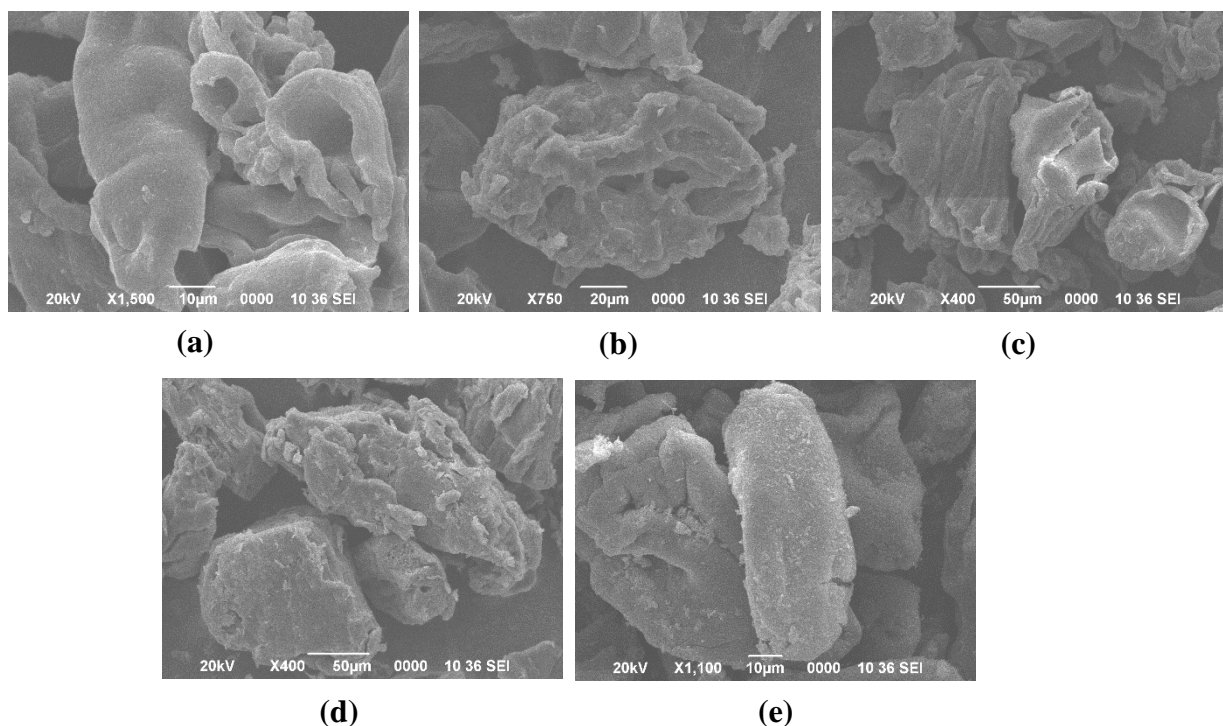


**Fig. 6.3.** SEM images of haritaki encapsulates obtained from freeze-drying (a) starch:zein (0:100) (b) starch:zein (30:70) (c) starch:zein (50:50) (d) starch:zein (70:30) (e) starch:zein (100:0)

The encapsulation powder's uniformity of microstructure after freeze-drying boosted its ability to protect phenolic chemicals [38]. The similar results were reported in the microcapsules loaded with phytochemicals of jabuticaba skin and seeds (*Myrciaria cauliflora*) [30].

### 6.3.5. FTIR Spectra of powder

The FT-IR spectra of native potato starch, which contained peaks at wave numbers of 1459, 1379, 1339, 1260, 1193, 1066, 1022, 939, and 867  $\text{cm}^{-1}$ , showed the presence of amylose and amylopectin (**Fig. 6.4**). All of these peaks were caused by the presence of different bonds, such as C-H, C-O-C, and O-H, which were anticipated using an IR chart. Bands in encapsulates samples that included various zein and starch quantities showed a little shifting. Zein and starch inclusion caused certain alterations that showed the presence of more amide bonds and OH groups in the insoluble fraction [41]. Ferreira-Villadiego et al. [17] also reported the existence of polysaccharides and C-H bending, respectively, was suggested by peaks at 1459 and 1350  $\text{cm}^{-1}$  and a vibration transmittance band between 1060 and 990  $\text{cm}^{-1}$ .

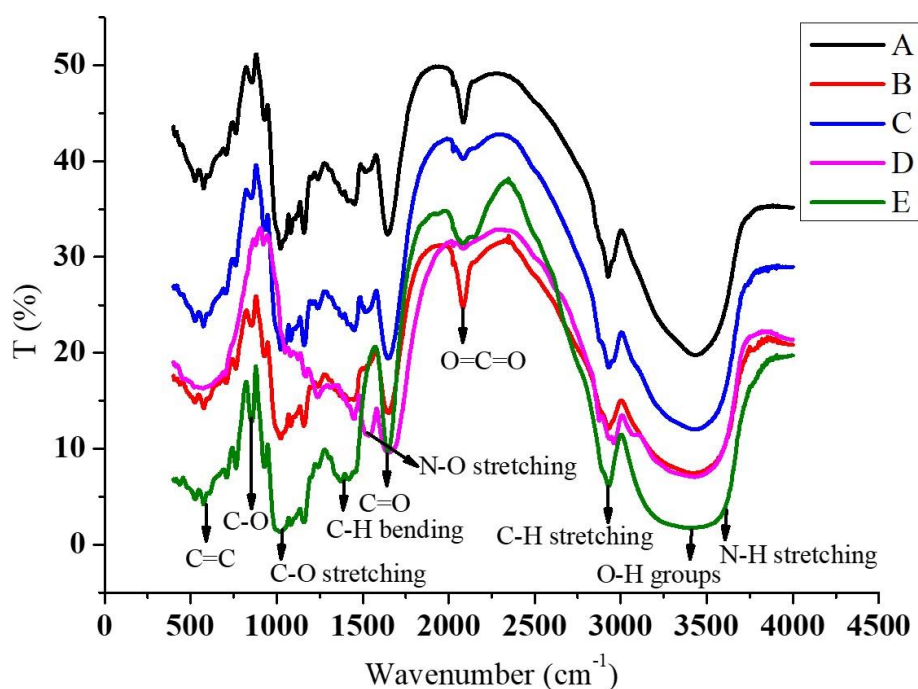


**Fig. 6.4.** FTIR spectra of encapsulates (A) starch:zein (0:100) (B) starch:zein (30:70) (C) starch:zein (50:50) (D) starch:zein (70:30) (E) starch:zein (100:0)

Ferreira-Villadiego et al. [17] also documented strain deformations of the C-O-C and flexion of the OH. The C-O-H deformation mode and CH<sub>2</sub>OH were both represented by the band at 1242 cm<sup>-1</sup>. On the other hand, the band at 1094 cm<sup>-1</sup> displayed the C-O-H bending modes, while the peak at 1163 cm<sup>-1</sup> appeared to be caused by the coupling of the C-O and C-C stretching modes. With all of the aforementioned, the CH<sub>2</sub> bending mode would have formed at 1344cm<sup>-1</sup> for the IR bands [10]. Others claimed that the carbon and hydrogen atoms were discovered to be linked to the vibrational bands (bending and deformation) that appeared in the range of 1500-1300 cm<sup>-1</sup> [45]. IR bands between 800-1200 cm<sup>-1</sup>, 1500-1200 cm<sup>-1</sup>, and 800-100 cm<sup>-1</sup> were discovered. While bands in the range of 1500-1200 cm<sup>-1</sup> and 800-100 cm<sup>-1</sup> were predominately dominated by the deformational modes of the CH/CH<sub>2</sub> and CO groups, respectively, it was proposed that these bands represented the stretching vibrations of the distinctive C-O and C-C groups. Similar to this, all starch samples infrared spectra showed peaks at 995-965 cm<sup>-1</sup> that looked to reflect ≡C-H bending and peaks at 867 cm<sup>-1</sup> that indicated the presence of certain Di substituted, Meta aromatic compounds with minor C-H bond stretching [32].

### 6.3.6. XRD

The XRD spectra of the freeze-dried haritaki capsule are represented in **Fig. 6.5**. The samples obtained with starch:zein (50:50) showcased dense diffraction peaks at  $17.5^\circ$  and weaker ones in-between  $19^\circ$  to  $25^\circ$ . Starch:zein (0:100), starch:zein (30:70) and starch:zein (100:0) had a slight intense diffraction at  $16^\circ$  whereas weak diffraction peak was observed in starch:zein (70:30). In general, zein levels in microcapsules decreased, and some peaks gradually vanished. Starch:zein microcapsules (50:50) only have a strong diffraction peak at  $17.5^\circ$ , indicating that the majority of the microcapsules were in an amorphous state. The amorphous state is often characterised by a higher water solubility. The similar result was displayed by Zhang et al. [53].

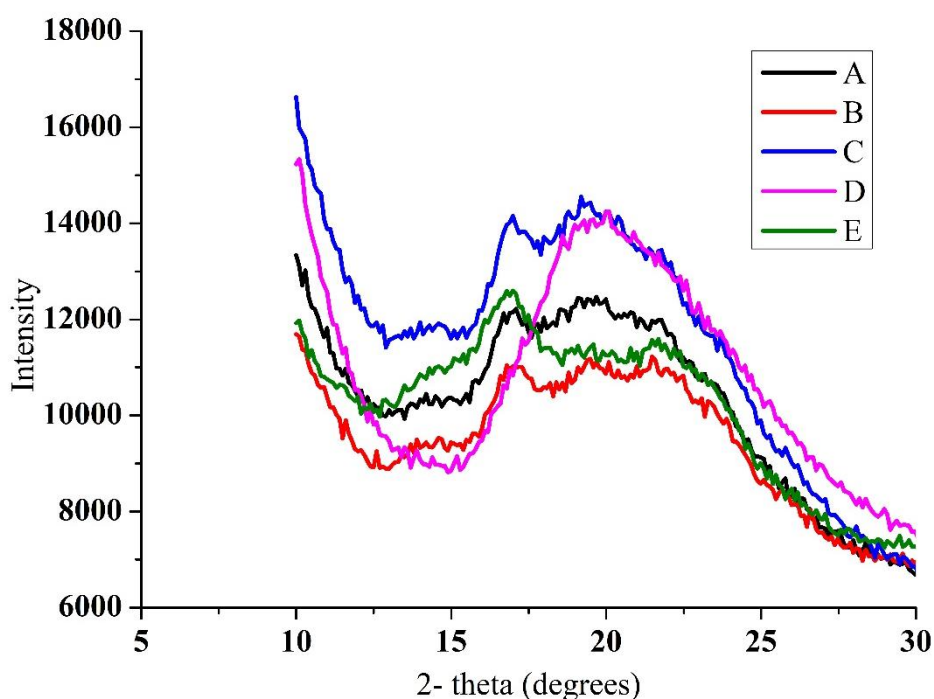


**Fig. 6.5.** XRD pattern of encapsulates (A) starch:zein (0:100) (B) starch:zein (30:70) (C) starch:zein (50:50) (D) starch:zein (70:30) (E) starch:zein (100:0)

### 6.3.7. Thermodynamic properties

#### 6.3.7.1. DSC

DSC results revealed significant change in the thermal parameters such as onset temperature ( $T_o$ ), peak temperature ( $T_p$ ), and conclusion temperature ( $T_c$ ) (**Table 6.2 and Fig. 6.6**). Encapsulates prepared using zein and starch varied concentration were gelatinized different temperature. The onset temperature ( $T_o$ ), peak temperature ( $T_p$ ), and

completion temperature ( $T_c$ ) of 100% zein encapsulate was 81.80, 114.80 and 142.70 °C respectively. The 100% starch encapsulate had a  $T_o$ ,  $T_p$ , and  $T_c$  of 83.90, 117.70 and 142.50 °C respectively. From the result it can be assumed that starch encapsulates required more temperature than zein encapsulate.

These results are in agreement with Irani et al. [21] and Pashazadeh et al. [38]. Gelatinization temperatures ( $T_o$ ,  $T_p$  and  $T_c$ ) and enthalpies of starches from various sources including corn, rice, wheat, and potato were found to be significantly different [48].

**Table 6.2.** Thermal properties and Mass loss of different encapsulates

<b>Parameters</b>	<b>A</b>	<b>B</b>	<b>C</b>	<b>D</b>	<b>E</b>
Onset temperature $T_o$ (°C)	81.80	87.30	88.40	77.70	83.90
Peak temperature $T_p$ (°C)	114.80	117.30	120.40	107.00	117.70
Conclusion temperature $T_c$ (°C)	142.70	138.10	138.70	122.30	142.50
<b>Mass Loss (%)</b>					
Decomposition (230- 350 °C)	58.63	62.06	62.82	68.12	67.23

The composition, shape, and ratio of the starch granules, as well as the amount of amylose and the amount of amylopectin, all affect the temperatures at which gelatinization occurs [12].

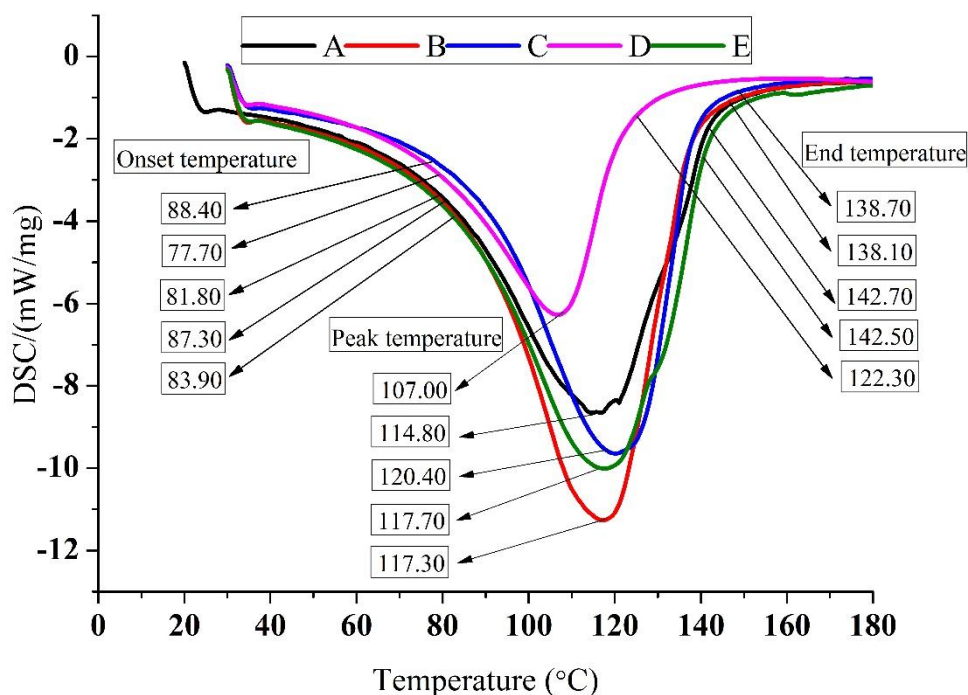


**Fig. 6.6.** Thermal properties of different encapsulates

With the addition of hydrocolloids, a decrease in the enthalpy of gelatinization was observed along with differences in the melting temperatures of numerous legume starches. The rate of amylopectin retrogradation, the amount of starch, and the temperature at which the food is finished heating all affect the aforementioned parameters.

### 6.3.7.2. TGA

Thermal deterioration is demonstrated via TGA by measuring mass loss as a function of temperature [8]. With the temperature rising (from 230 to 350 °C), volatile chemicals in the encapsulates immediately began to evaporate, which is why the first weight loss was noticed (**Table 6.2 and Fig. 6.7**). During TGA, various temperature ranges had an impact on how various materials performed. The first mass loss did not vary significantly as encapsulate composition increased.



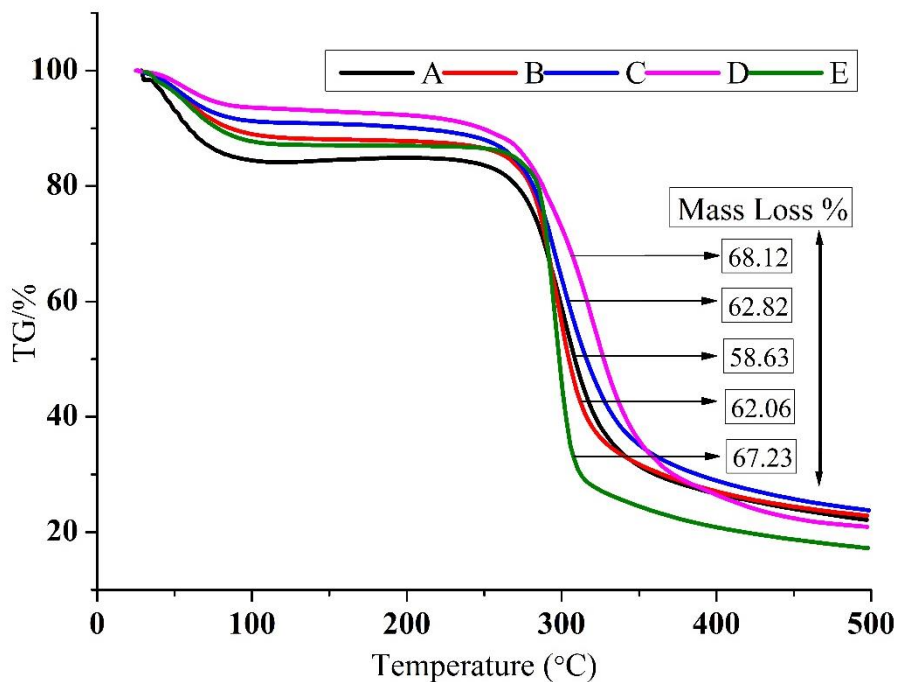


**Fig. 6.7.** Mass loss of different encapsulates

Maximum mass loss was observed in 70:30 (starch:zein) encapsulates followed by 100% starch encapsulates. There were no significant difference were recorded in 30:70 (starch:zein) and 50:50 (starch:zein) encapsulates. Previous studies suggested that the first stage of weight loss was similar to the physical dehydration of starch, while the second stage entailed chemical and thermal degradation [2]. At the third stage, chemical oxidation caused weight loss, which resulted in varied mass losses at temperatures between 300 and 400 °C. This stage, which is a combustion stage, is what completely oxidised the organic materials. According to Malumba et al. [29], at this point, a sharp loss in mass was seen as a result of the release of volatile compounds, this could have been caused by the release of water molecules, other tiny molecular species, the synthesis of additional carbonaceous residues, and heat condensation between the hydroxyl groups of the starch chains to create either segment. According to the results of the TGA on the encapsulates, thermal degradation took place between 230 and 350 °C. Depending on the concentration, the ratio of the starch's amylose and amylopectin contents and their interaction with the protein zein may result in varying heat stability and distinct disintegration mechanisms [49].

#### 6.4. Conclusion

Haritaki extract was successfully encapsulated using the different combination of starch and zein by means of freeze-drying. Different combinations of starch:zein was tried to encapsulate the bioactive compound and based on the yield, encapsulation efficiency, and powder density, 100% starch encapsulates presented better results among the combinations. From the SEM study, it was verified that encapsulates had a rough and irregular shape. TGA study revealed the maximum loss in mass in the 70:30 (starch:zein) combination while the minimum mass loss occurred in 100% zein. From DSC curves, it was noticed that the maximum onset point and peak point were presented by 50:50 (starch:zein) encapsulates, while the minimum onset point and peak point were depicted by 70:30 (starch:zein) encapsulates. The maximum endpoint was seen in 100% starch encapsulates whereas 30:70 (starch:zein) encapsulates showed a minimum value. FTIR spectra revealed that 100% zein encapsulates had maximum stretching and vibrations in the bond while encapsulates prepared from 100% starch had very minimum stretching and poor intensities in bonds. XRD pattern detailed that, no sharpness in the encapsulates except 50:50 (starch:zein). The encapsulation process of haritaki was initiated by the chemical interaction between the composite wall materials (starch and zein) in an amorphous state, and authenticated by FTIR and XRD. Haritaki could also be promoted as a stable bioactive compound and functional ingredient in the clean-label food industry. Also, the encapsulates can be valorized for the development of functional products.

## 6.5. References

1. Aceval Arriola, N. D., De Medeiros, P. M., Prudencio, E. S., Olivera Müller, C. M., and De Mello Castanho Amboni, R. D. Encapsulation of aqueous leaf extract of *Stevia rebaudiana* Bertoni with sodium alginate and its impact on phenolic content. *Food Bioscience*, 13, 32–40, 2016.
2. Acevedo, L. A., Korson, N. E., Williams, J. M., and Nicholson, L. K. Tuning a timing device that regulates lateral root development in rice. *Journal of biomolecular NMR*, 73(8), 493-507, 2019.
3. Alehosseini, A., Ghorani, B., Sarabi-Jamab, M., and Tucker, N. Principles of electrospraying: A new approach in protection of bioactive compounds in foods. *Critical reviews in food science and nutrition*, 58(14), 2346-2363, 2018.
4. Álvarez-Henao, M. V., Saavedra, N., Medina, S., Cartagena, C. J., Alzate, L. M., and Londoño-Londoño, J. Microencapsulation of lutein by spray-drying: Characterization and stability analyses to promote its use as a functional ingredient. *Food Chemistry*, 256, 181-187, 2018.
5. Arriola, N. D. A., de Medeiros, P. M., Prudencio, E. S., Müller, C. M. O., and Amboni, R. D. D. M. C. Encapsulation of aqueous leaf extract of *Stevia rebaudiana* Bertoni with sodium alginate and its impact on phenolic content. *Food Bioscience*, 13, 32-40, 2016.
6. Bashir, K., and Aggarwal, M. Effects of gamma irradiation on the physicochemical, thermal and functional properties of chickpea flour. *LWT-Food Science and Technology*, 69, 614-622, 2016.
7. Bashir, M., and Haripriya, S. Assessment of physical and structural characteristics of almond gum. *International Journal of Biological Macromolecules*, 93, 476-482, 2016.
8. Bet, C. D., de Oliveira, C. S., Beninca, C., Colman, T. A. D., Lacerda, L. G., and Schnitzler, E. Influence of the addition of hydrocolloids on the thermal, pasting and structural properties of starch from common vetch seeds (*Vicia sativa* sp). *Journal of Thermal Analysis and Calorimetry*, 133(1), 549-557, 2018.
9. Botrel, D. A., de Barros Fernandes, R. V., Borges, S. V., and Yoshida, M. I. Influence of wall matrix systems on the properties of spray-dried microparticles containing fish oil. *Food Research International*, 62, 344-352, 2014.

10. Cael, J. J., Koenig, J. L., and Blackwell, J. Infrared and Raman spectroscopy of carbohydrates. Part VI: Normal coordinate analysis of V-amylase. *Biopolymers: Original Research on Biomolecules*, 14(9), 1885-1903, 1975.
11. Çam, M., İçyer, N. C., and Erdoğan, F. Pomegranate peel phenolics: Microencapsulation, storage stability and potential ingredient for functional food development. *LWT-Food Science and Technology*, 55(1), 117-123, 2014.
12. Chang, P. R., Jian, R., Zheng, P., Yu, J., and Ma, X. Preparation and properties of glycerol plasticized-starch (GPS)/cellulose nanoparticle (CN) composites. *Carbohydrate Polymers*, 79(2), 301-305, 2010.
13. Das, D., Das, D., Gupta, A. K., and Mishra, P. Drying of citrus grandis (pomelo) fruit juice using block freeze concentration and spray drying. *Acta Alimentaria*, 49(3), 295-306, 2020.
14. de Cássia Sousa Mendes, D., Asquieri, E. R., Batista, R. D., de Moraes, C. C., Ramirez Ascheri, D. P., and de Macêdo, I. Y. L. Microencapsulation of jabuticaba extracts (*Myrciaria cauliflora*): Evaluation of their bioactive and thermal properties in cassava starch biscuits. *Lwt- Food Science and Technology*, 137, 2021.
15. Edris, A. E., Kalembe, D., Adamiec, J., and Piątkowski, M. Microencapsulation of *Nigella sativa* oleoresin by spray drying for food and nutraceutical applications. *Food Chemistry*, 204, 326-333, 2016.
16. Elzoghby, A. O., Samy, W. M., and Elgindy, N. A. Protein-based nanocarriers as promising drug and gene delivery systems. *Journal of controlled release*, 161(1), 38-49, 2012.
17. Ferreira-Villadiego, J., Garcia-Echeverri, J., Mejia, M. V., Pasqualino, J., Meza-Catellar, P., and Lambis, H. Chemical modification and characterization of starch derived from plantain (*Musa paradisiaca*) Peel waste, as a source of biodegradable material. *Chemical Engineering Transactions*, 65, 763-768, 2018.
18. Fu, T. J., Abbott, U. R., and Hatzos, C. Digestibility of food allergens and nonallergenic proteins in simulated gastric fluid and simulated intestinal fluid a comparative study. *Journal of agricultural and food chemistry*, 50(24), 7154-7160, 2002.
19. Gaona-Sánchez V. A., Calderón-Domínguez G., Morales-Sánchez E., Chanona-Pérez J. J., Velázquez-de la Cruz G., and Méndez-Méndez J. V. Preparation and characterisation of zein films obtained by electrospraying. *Food Hydrocolloids*, 49:1–10, 2015.

20. Gómez-Mascaraque, L. G., Perez-Masiá, R., González-Barrio, R., Periago, M. J., and López-Rubio, A. Potential of microencapsulation through emulsion-electrospraying to improve the bioaccessibility of  $\beta$ -carotene. *Food Hydrocolloids*, 73, 1-12, 2017.
21. Irani, M., Sadeghi, G. M. M., and Haririan, I. A novel biocompatible drug delivery system of chitosan/temozolomide nanoparticles loaded PCL-PU nanofibers for sustained delivery of temozolomide. *International journal of biological macromolecules*, 97, 744-751, 2017.
22. Jain, A., Sharma, G., Kushwah, V., Ghoshal, G., Jain, A., Singh, B., and Katare, O. P. Beta carotene-loaded zein nanoparticles to improve the biopharmaceutical attributes and to abolish the toxicity of methotrexate: A preclinical study for breast cancer. *Artificial cells, nanomedicine, and biotechnology*, 46, 402-412, 2018.
23. Jha, A. K., and Sit, N. Comparison of response surface methodology (RSM) and artificial neural network (ANN) modelling for supercritical fluid extraction of phytochemicals from Terminalia chebula pulp and optimization using RSM coupled with desirability function (DF) and genetic algorithm (GA) and ANN with GA. *Industrial Crops and Products*, 170, 113769, 2021.
24. Jha, A. K., Kumari, S., Gupta, A. K., and Shashank, A. Improvement in pasting, thermal properties, and in vitro digestibility of isolated Amaranth starch (*Amaranthus cruentus* L.) by addition of almond gum and gum ghatti powder. *Journal of Food Processing and Preservation*, 45(10), 2021.
25. Khazaei, K. M., Jafari, S. M., Ghorbani, M., and Kakhki, A. H. Application of maltodextrin and gum Arabic in microencapsulation of saffron petal's anthocyanins and evaluating their storage stability and color. *Carbohydrate polymers*, 105, 57-62, 2014.
26. Kuck, L. S., and Noreña, C. P. Z. Microencapsulation of grape (*Vitis labrusca* var. Bordo) skin phenolic extract using gum Arabic, polydextrose, and partially hydrolyzed guar gum as encapsulating agents. *Food chemistry*, 194, 569-576, 2016.
27. Kumar, A., Kumar, S., Rai, A., and Ram, B. Pharmacognostical and Phytochemical Evaluation of haritaki (*Terminalia chebula* Retz.) fruit pulp. *International Journal of Pharmaceutical, Chemical & Biological Sciences*, 7(4), 2017.
28. Mahalakshmi, L., Leena, M. M., Moses, J. A., and Anandharamakrishnan, C. Micro- and nano-encapsulation of  $\beta$ -carotene in zein protein: Size-dependent release and absorption behavior. *Food & function*, 11(2), 1647-1660, 2020.

29. Malumba, P., Bungu, M. D., Katanga, K. J., Doran, L., Danthine, S., and Béra, F. Structural and physicochemical characterization of *Sphenostylis stenocarpa* (Hochst. ex A. Rich.) Harms tuber starch. *Food Chemistry*, 212, 305-312, 2016.
30. Mendes, D. D. C. S., Asquieri, E. R., Batista, R. D., de Morais, C. C., Ascheri, D. P. R., de Macêdo, I. Y. L., and de Souza Gil, E. Microencapsulation of jaboticaba extracts (*Myrciaria cauliflora*): Evaluation of their bioactive and thermal properties in cassava starch biscuits. *Lwt- Food Science and Technology*, 137, 110460, 2021.
31. Mishra, P., and Kar, R. Treatment of grapefruit juice for bitterness removal by Amberlite IR 120 and Amberlite IR 400 and alginate entrapped naringinase enzyme. *Journal of Food Science*, 68(4), 1229-1233, 2003.
32. Mohrig, J. R., Hammond, C. N., and Schatz, P. F. *Techniques in organic chemistry*. Macmillan, 2010.
33. Moreira, G. E. G., Costa, M. G. M., de Souza, A. C. R., de Brito, E. S., de Medeiros, M. D. F. D., and de Azeredo, H. M. Physical properties of spray dried acerola pomace extract as affected by temperature and drying aids. *LWT-Food Science and Technology*, 42(2), 641-645, 2009.
34. Moreira, G. É. G., DE Azeredo, H. M. C., DE Medeiros, M. D. F. D., De Brito, E. S., and DE Souza, A. C. R. Ascorbic acid and anthocyanin retention during spray drying of acerola pomace extract. *Journal of Food Processing and Preservation*, 34(5), 915-925, 2010.
35. Nayak, A. K., Hasnain, M. S., Dhara, A. K., and Mandal, S. C. Herbal biopolysaccharides in drug delivery. In *Herbal biomolecules in healthcare applications* (pp. 613-642). Academic Press, 2022.
36. Negrão-Murakami, A. N., Nunes, G. L., Pinto, S. S., Murakami, F. S., Amante, E. R., Petrus, J. C. C., and Amboni, R. D. Influence of DE-value of maltodextrin on the physicochemical properties, antioxidant activity, and storage stability of spray dried concentrated mate (*Ilex paraguariensis* A. St. Hil.). *LWT-Food Science and Technology*, 79, 561-567, 2017.
37. Nunes, G. L., Boaventura, B. C. B., Pinto, S. S., Verruck, S., Murakami, F. S., Prudêncio, E. S., and Amboni, R. D. D. M. C. Microencapsulation of freeze concentrated *Ilex paraguariensis* extract by spray drying. *Journal of Food Engineering*, 151, 60-68, 2015.
38. Pashazadeh, H., Zannou, O., Ghellam, M., Koca, I., Galanakis, C. M., and Aldawoud, T. M. Optimization and Encapsulation of Phenolic Compounds Extracted from Maize

- Waste by Freeze-Drying, Spray-Drying, and Microwave-Drying Using Maltodextrin. *Foods*, 10(6), 1396, 2021.
39. Pramodrao, K. S., and Riar, C. S. Comparative study of effect of modification with ionic gums and dry heating on the physicochemical characteristic of potato, sweet potato and taro starches. *Food Hydrocolloids*, 35, 613-619, 2014.
  40. Rathinamoorthy, R., and Thilagavathi, G. Optimisation of process conditions of cotton fabric treatment with Terminalia chebula extract for antibacterial application, 2013.
  41. Rezaei, A., Nasirpour, A., and Tavanai, H. Fractionation and some physicochemical properties of almond gum (*Amygdalus communis* L.) exudates. *Food Hydrocolloids*, 60, 461-469, 2016.
  42. Rezende, Y. R. R. S., Nogueira, J. P., and Narain, N. Microencapsulation of extracts of bioactive compounds obtained from acerola (*Malpighia emarginata* DC) pulp and residue by spray and freeze drying: Chemical, morphological and chemometric characterization. *Food Chemistry*, 254, 281-291, 2018.
  43. Santhalakshmy, S., Bosco, S. J. D., Francis, S., and Sabeena, M. Effect of inlet temperature on physicochemical properties of spray-dried jamun fruit juice powder. *Powder Technology*, 274, 37-43, 2015.
  44. Santos, S. S., Rodrigues, L. M., Da Costa, S. C., Bergamasco, R. D. C., and Madrona, G. Microcapsules of blackberry pomace (*Rubus fruticosus*): Light and temperature stability. *Chemical Engineering Transactions*, 57, 1837-1842, 2017.
  45. Schuster, K. C., Ehmoser, H., Gapes, J. R., and Lendl, B. On-line FT-Raman spectroscopic monitoring of starch gelatinisation and enzyme catalysed starch hydrolysis. *Vibrational Spectroscopy*, 22(1-2), 181-190, 2000.
  46. Shang, M., Wang, W., Sun, S., Gao, E., Zhang, Z., Zhang, L., and O'Hayre, R. The design and realization of a large-area flexible nanofiber-based mat for pollutant degradation: an application in photocatalysis. *Nanoscale* 5, 5036–5042, 2013.
  47. Silva, P. I., Stringheta, P. C., Teófilo, R. F., and de Oliveira, I. R. N. Parameter optimization for spray-drying microencapsulation of jaboticaba (*Myrciaria jaboticaba*) peel extracts using simultaneous analysis of responses. *Journal of Food Engineering*, 117(4), 538-544, 2013.
  48. Singh, N., Singh, J., Kaur, L., Sodhi, N. S., and Gill, B. S. Morphological, thermal and rheological properties of starches from different botanical sources. *Food chemistry*, 81(2), 219-231, 2003.

49. Soares, R. M. D., Lima, A. M. F., Oliveira, R. V. B., Pires, A. T. N., and Soldi, V. Thermal degradation of biodegradable edible films based on xanthan and starches from different sources. *Polymer degradation and stability*, 90(3), 449-454, 2005.
50. Suriya, M., Baranwal, G., Bashir, M., Reddy, C. K., and Haripriya, S. Influence of blanching and drying methods on molecular structure and functional properties of elephant foot yam (*Amorphophallus paeoniifolius*) flour. *LWT-Food Science and Technology*, 68, 235-243, 2016.
51. Susantikarn, P., and Donlao, N. Optimization of green tea extracts spray drying as affected by temperature and maltodextrin content. *International Food Research Journal*, 23(3), 1327, 2016.
52. Wiercigroch, E., Szafraniec, E., Czamara, K., Pacia, M. Z., Majzner, K., Kochan, K., and Malek, K. Raman and infrared spectroscopy of carbohydrates: A review. *Spectrochimica Acta Part A: Molecular and Biomolecular Spectroscopy*, 185, 317-335, 2017.
53. Zhang, T., Yu, S., Tang, X., Ai, C., Chen, H., Lin, J., and Guo, X. Ethanol-soluble polysaccharide from sugar beet pulp for stabilizing zein nanoparticles and improving encapsulation of curcumin. *Food Hydrocolloids*, 124, 107208, 2022.